

A&A manuscript no.
(will be inserted by hand later)

Your thesaurus codes are:
09.03.2; 10.03.1; 13.07.2; 13.07.3

**ASTRONOMY
AND
ASTROPHYSICS**
23.9.2018

The galactic center arc as source of high energy γ -rays

M. Pohl

Max-Planck-Institut für Extraterrestrische Physik, Postfach 1603, 85740 Garching, Germany

[the date of receipt and acceptance should be inserted later]

Abstract. In this paper we discuss the radio *arc* at the galactic center to be the counterpart of the high-energy γ -ray source 2EG J1746-2852.

Though 2EG J1746-2852 must be regarded as true source in excess of the diffuse background, its position can not be determined to better than 0.3° . The observed flux is constant within the statistical limits and the spectrum is very hard. The lack of variability makes it highly unlikely that any of the compact sources in the vicinity of the Galactic Center is the counterpart of 2EG J1746-2852. This includes the peculiar source Sgr A* at the very center of the Galaxy, which is often discussed to harbour a black hole of $10^6 M_\odot$.

Existing radio data on the *arc* support the view that its synchrotron emission originates from cooling, initially monoenergetic electrons which diffuse and convect from their sources to the outer extensions of the *arc*. If the source of high-energy electrons coincides with the sickle region (G0.18-0.04), as indicated by the radio data, then the ambient far-infrared (FIR) photons can be up-scattered to γ -rays by inverse-Compton interaction with the young high-energy electrons. We solve the continuity equation for the electrons including terms for diffusion, convection, monoenergetic injection, and the full energy loss. With that we show that the predicted γ -ray emission depends mainly on the magnetic field strength in the *arc* and that both the flux and the spectrum of 2EG J1746-2852 can be well explained. Our model shall be tested on radio data at frequencies beyond 10 GHz in future work.

Key words: Cosmic Rays - Galactic Center - Gamma Rays

1. The Galactic center region

Early radio studies of the galactic center region have revealed the source Sgr A located at the mass and dynamical center of the Galaxy. Sgr A has been observed at the highest angular resolution presently obtainable for a wide range of wavelengths. The main component of Sgr A is the extremely compact discrete source Sgr A*, which is located close to the center of the

spirallike thermal source Sgr A West. Sgr A* is unique in the Galaxy and shows a similar behaviour like active galactic nuclei although its luminosity is orders of magnitudes less. VLBI observations at 43 GHz and 86 GHz indicate a size of a few Astronomical Units or less (Krichbaum et al. 1993). Sgr A* is variable and has an inverted synchrotron spectrum close to $\alpha=0.3$ ($S \propto \nu^\alpha$), which may originate from nearly monoenergetic electrons. At X-ray energies a strongly variable source coinciding with Sgr A* has been reported (Skinner et al. 1987, Sunyaev et al. 1991, Churazov et al. 1994). However, deep high-resolution observations indicate that Sgr A* itself is a weak emitter (Predehl and Trümper 1994, for a discussion see Goldwurm et al. 1994).

Within 50 pc of Sgr A two more components are located, which are significantly weaker and referred to as the *arc* and the *bridge*. Recombinations lines detected from the emission of the *bridge* indicate the existence of thermal material, while the detection of polarized emission from the *arc* region and the absence of recombinations lines show the dominance of synchrotron radiation from this region. The magnetic field has been shown to run parallel to the *arc* with a very high degree of regularity by 32 GHz observations (Reich 1990) and 43 GHz (Tsuboi et al. 1995). High resolution observations with the VLA have revealed a number of long and very thin filaments superimposed on the diffuse emission of the *arc* as well as isolated threads distributed throughout the galactic center region. The isolated threads have normal steep radio spectra $\alpha \approx -0.5$ ($S \propto \nu^\alpha$). The filaments in the *arc* have inverted spectra with $\alpha \simeq 0.3$ at 1 GHz (Anantharamiah et al. 1991), while they are hardly seen at 43 GHz, implying a steep spectral index $\alpha \simeq -0.7$ between 5 GHz and 43 GHz (Sofue, Murata and Reich 1992). At 43 GHz the filaments contribute less than 10% to the total brightness of the *arc*. Given the inverted spectrum of the total emission of the *arc* up to 43 GHz (Reich et al. 1988) and the high degree of polarization at 32 GHz and 43 GHz, a substantial amount of diffuse synchrotron emission with inverted spectrum is required. The *arc* extends northward and southward to plumes with high degree of polarization but steeper spectrum. These extensions may be understood as due to ageing, initially monoenergetic electrons, which have been transported by diffusion and convection from their sources in the *arc* (Pohl, Reich and Schlickeiser 1992,

Send offprint requests to:

<http://www.gamma.mpe-garching.mpg.de/~mkp/mkp.html>

abbreviated as **PRS**), although a detailed modelling suffered from systematical uncertainties in the data set.

2. EGRET results for the galactic center

The EGRET instrument on the Compton Gamma-Ray Observatory is sensitive to γ -rays in the energy range of 30 MeV to 30 GeV. The instrument design is described in Kanbach et al. (1988) and information on the instrument calibration may be found in Thompson et al. (1993). For point sources a maximum likelihood analysis (Mattox et al. 1996) is used to determine the number of source photons, distributed according to the instrument point spread function, in excess to a model parametrisation of the galactic diffuse background emission.

With this technique a highly significant γ -ray source (2EG J1746-2852) was found to be positionally coincident with the galactic center (Thompson et al. 1996). There is a weak preference for a source position at $\approx 0.2^\circ$, especially at high γ -ray energies (> 1 GeV), although the exact center position or even a negative longitude can not be ruled out completely. Its integrated flux above 100 MeV is around 10^{-6} ph./cm²/sec.

Some uncertainties in the background model near the galactic center demand a careful analysis of the data, which in its full scope will be published elsewhere (Mayer-Häselwander et al., in prep.). Here we give a short overview on the basic results which are of relevance for our modelling.

2.1. Variability

The γ -ray light curve at photon energies above 100 MeV of 2EG J1746-2852 between April 1991 and September 1993 has already been published in Thompson et al. (1996). There is no evidence for variability during this period of time. We have further analysed public data of Phase 3 (September 1993 to October 1994) and find no evident sign of variability either. Therefore we conclude that the EGRET results of Phase 1 to Phase 3 are well compatible with 2EG J1746-2852 being a constant emitter of γ -rays.

2.2. The spectrum

The γ -ray spectrum in the EGRET range has been determined on the basis of summed data sets of Phase 1 and Phase 2 by Merck et al. (1996). It appears to be well represented by a hard power-law with a cut-off at a few GeV, hence is significantly different from that of the galactic diffuse emission, but resembles the spectra of γ -ray pulsars. Neglecting the highest energy bin (4 GeV to 10 GeV) the photon spectral index is $s = -1.6 \pm 0.09$ ($I = I_0 E^s$).

We can also use COMPTEL data at lower energies (Strong, priv. comm.). Since COMPTEL's limited angular resolution does not allow to discriminate between a point source at the galactic center and continuum emission from the galactic center molecular arm, the final flux values were taken as upper limits for the galactic center source for systematic reasons. The resulting total spectrum will be shown in Fig.2.

2.3. Discussion of EGRET results

To summarize, 2EG J1746-2852 is a steady source of high energy γ -rays with a very hard spectrum.

One possible counterpart is Sgr A*. Standard models for the emission of accreting matter around a massive black hole predict negligible γ -ray emission (Narayan et al. 1996, Melia 1994). However, high energy emission may arise from shock accelerated protons in the vicinity of the black hole (Mastichiadis and Ozeroy 1994). In the latter model X-rays are produced by synchrotron radiation of secondary electrons. These electrons can not at the same time be responsible for the radio and near-infrared (NIR) emission since the cooling spectrum of secondary electrons below 100 MeV is incompatible with the observed spectrum in the mm-range. Also, if the gas densities are not higher than 10^7 cm⁻³, the source should be constant in X-rays and γ -rays.

However, Sgr A* is observed to be variable at X-ray energies and in the radio regime, and it is highly unlikely that it remains constant in the energy range in which it would have to emit its peak of luminosity and in which the physical time scales are shortest, at γ -ray energies. Therefore we consider it unlikely that Sgr A* or any other compact source in the galactic center vicinity is the counterpart to 2EG J1746-2852.

A misinterpretation of strong diffuse emission as point source can be excluded on the basis of the source spectrum and the incompatibility of its structure with the spatial distribution of gas, which forms a ridge of 1.5° length (Sofue 1995a,b). To account for the observed flux the γ -ray emissivity per H-atom at the galactic center molecular arm would have to be 5-10 times larger than the local value.

The γ -ray spectrum of 2EG J1746-2852 resembles that of a pulsar, possibly of Geminga type. There is no radio pulsar known to be positionally consistent with 2EG J1746-2852 (Taylor et al. 1993). Given the γ -ray luminosity of Geminga a similar pulsar would have to be within a few hundred parsecs distance to produce the observed γ -ray flux of 2EG J1746-2852. This γ -ray source however is the only yet unidentified EGRET source which has a spectrum compatible with an old γ -ray pulsar (Merck et al. 1996), hence it would be extremely unlikely ($P \approx 10^{-5}$) that such a hypothetical γ -ray pulsar is located positionally consistent with the Galactic center.

A remaining promising candidate for the counterpart of 2EG J1746-2852 is the galactic center *arc* in which relativistic electrons exist with unusually hard spectrum. Based on radio data at frequencies of 10 GHz and less **PRS** have modelled the radio emission of the *arc* as synchrotron emission of initially monoenergetic electrons, which propagate along the magnetic field and thereby loose their energy to adiabatic expansion and radiation processes. This basic scenario is supported by recently published 43 GHz data (Tsuboi et al. 1995), which show flat spectra between 10 GHz and 43 GHz at -3° latitude in the *arc* and spectral softening towards the outer extensions. In detail the modelling in **PRS** was hampered by uncertainties in the contribution of localized thermal emission, especially at the 'sickle', and in the relation of the (in single-dish data unresolved) filaments to the diffuse synchrotron emission, which

both influence the local relation of flux density and spectral index. Signatures of these systematics are the weak polarization where the thermal arches cross the *arc* and the shift of the peak flux density towards lower galactic longitudes with frequency (Reich et al. 1988).

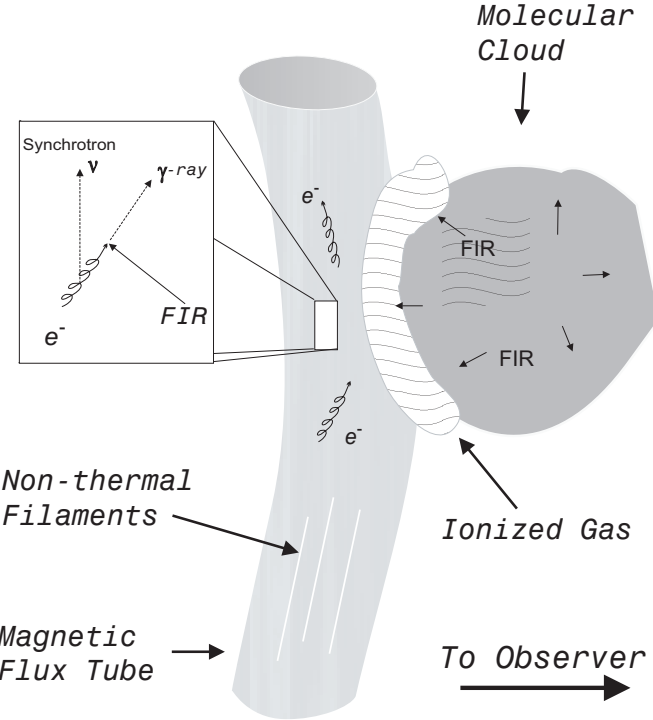


Fig. 1. Sketch of the basic scenario. A molecular clouds (M0.20-0.033) presses on a magnetic flux tube (the *arc*) with an HII region (G0.18-0.04) as contact interface. Narrow non-thermal filaments with inverted radio spectrum up to 5 GHz are imbedded in the flux tube. The flux tube itself is filled also with diffuse high-energy electrons which reveal themselves by synchrotron radiation inverted spectrum at least up to 43 GHz. The most energetic electrons can up-scatter FIR photons emitted by the molecular cloud complex to γ -rays .

The HII region G0.18-0.04 (the 'sickle') is probably located in front of the filaments in the *arc* (Lasenby et al. 1989). G018-0.04 appears to be represent the interaction zone between the dense molecular cloud M0.20-0.033 and the magnetic field structure of the *arc*. Based on the spatial coincidence of molecular clumps with the endpoints of filaments Serabyn and Morris (1994) have argued that these interaction regions are the acceleration sites for the relativistic electrons in the *arc*. Interestingly, the total FIR luminosity in the G0.18-0.04/M0.20-0.033 interface region is nearly $10^7 L_\odot$ (Odenwald and Fazio 1984). These FIR photons may be inverse Compton scattered to become γ -rays . The basic scenario is displayed as sketch in Fig.1, where the insert shows the radiation processes of the high-energy electrons: synchrotron radiation and up-scattering of the FIR photons emitted by the molecular cloud complex M0.20-0.033.

The observed γ -ray spectrum of 2EG J1746-2852 requires an E^{-2} electron spectrum which is the natural consequence of cooling, initially monoenergetic electrons, harmonizing with

what is required to explain the synchrotron data. In the next section we will briefly discuss the evolution of monoenergetic particle spectra, before in section 4 we test whether the flux ratios of γ -rays to synchrotron photons from the *arc* are compatible with the data.

3. The build-up and evolution of monoenergetic spectra

Monoenergetic particle spectra may arise from acceleration by magnetic reconnection (Kaastra 1985) or from the concerted action of first and second order Fermi acceleration, synchrotron and inverse Compton losses, and escape (Schlickeiser 1984). Here we restrict our discussion on the evolution of such monoenergetic spectra after the particles have escaped from the acceleration zone, independent of the acceleration process. The injection rate of monoenergetic particles is assumed to be constant. Then the evolution of such particles is well described by a one-dimensional continuity equation (see Appendix A, eq. A1) containing terms for spatial diffusion, convection in an accelerated flow, and all energy loss processes. Such an equation can be solved analytically. The solution for low-density environments (no bremsstrahlung, no ionisation and Coulomb losses) can be found in PRS while the general result is given in the Appendix A.

The volume-integrated electron spectrum is basically the inverse of the energy loss term. The spectral index is 0 at low energies where ionisation and Coulomb losses dominates. It changes to -1 at medium energies where adiabatic deceleration and bremsstrahlung losses dominate while being -2 at high energies due to the influence of synchrotron and inverse Compton losses. The spectrum extends up to the injection energy.

The differential number density of electrons, i.e. the local spectrum, has a more complicated behaviour. If the injection of electrons occurs only at the symmetry point of the large-scale convection flow, then the spatial extent of the particle distribution is a simple function of electron energy. It increases as $E^{(a-1)/2}$ at high energies, where a is the power-law exponent of the diffusion coefficient. At medium energies the behaviour depends on the relative strength of bremsstrahlung losses and adiabatic cooling. The spatial extent increases as E^{-3} if only adiabatic losses are operating, is independent of energy if only bremsstrahlung losses are efficient, and is in between in the general case. At low energies the spatial extent is always independent of energy. Therefore, the spectral index of the differential number density within the confinement volume is 0 at low energies, $-(3+a)/2$ at high energies, and varying between 2 and -1 at medium energies.

A spatially extended source affects strongly the low energy spectra even at larger distances from the source region, if the source region is larger than the spatial extent of the particle distribution at the transition energy E_D between dominance of radiative losses and dominance of adiabatic cooling and bremsstrahlung in case of a point-like origin. This may be part of the reason why a detailed modelling of the radio flux density and spectral index remained inconclusive. However, this problem does not affect the high energy γ -ray emission, since

the target photons for inverse Compton scattering are not so concentrated as the highest energy electrons. Therefore in high energy γ -rays we see all electrons (i.e. the volume-integrated spectrum), provided the sources of electrons are located within the region of high FIR photon density. The particle spectral index of -2 than translates to a photon spectral index of -1.5 for the inverse-Compton emission.

4. Modelling of the γ -ray source

From the emission measure of the thermal gas within the HII -region G0.18-0.04 we obtain a density $n_e \simeq 100$ of ionized material. The molecular cloud M0.20-0.033 has densities $n_H \geq 10^4$ in its core as traced by CS line observations (Serabyn and Morris 1994). The atomic and molecular gas will be at least partly external to the *arc* and to the relativistic electrons confined to it. Bremsstrahlung arising from the interaction of relativistic electrons with this thermal matter plays only a minor role and is not able to account for the observed γ -ray flux. However, interactions with the gas have impact on the evolution of the cooling electrons due to the corresponding energy losses. We have allowed for some thermal gas inside the *arc* with a density small enough so that it does not dominate the electron energy loss. Our analytical solution of the electron transport equation requires the energy loss terms not to vary with position. Generally a gas density of $n \leq 100 \text{ cm}^{-3}$ was found to be consistent with adiabatic losses dominating over bremsstrahlung. The examples in this section are calculated for $n = 50 \text{ cm}^{-3}$. Variation of this number leads to changes in the prediction for the flux and spectral index distribution of the radio emission, but leaves the high energy γ -ray emission unaffected. The impact on the radio emission can partly be counterbalanced by adjusting the magnetic field strength and the electron source geometry. A similar argument applies to the high-energy regime where the energy losses due to inverse-Compton scattering should be smaller than those due to synchrotron emission which requires $B \geq 60 \mu\text{G}$. Our example below is calculated for $B = 200 \mu\text{G}$.

The interesting γ -ray production process is inverse Compton scattering on the ambient FIR photons. Given an FIR luminosity at the G0.18-0.04/M0.20-0.033 interface of $10^7 L_\odot$ (Morris, Davidson and Werner 1995; Davidson, priv. comm.) the average photon energy density is around 100 eV/cm^3 for a spherical region of 8 pc radius. The spectrum is assumed to be grey-body with a temperature of 50 K, harmonizing with the surface brightness ratio at $50 \mu\text{m}$ and $90 \mu\text{m}$ (Morris, Davidson and Werner 1995). The flux of γ -rays due to this process is high if the source region of electrons coincides with or is near to the FIR emission region since the required electrons of 100 GeV energy can not propagate far before loosing their energy. Due to the short energy loss time scales at these energies this assumption also implies that we see all electrons at high energies, hence the electron spectral index is -2 up to the injection energy.

Since the photon source is external to the *arc* the photon distribution cannot be regarded as isotropic. In our modelling we approximate the molecular cloud M0.20-0.033 as point

source of FIR photons located at a distance $R_0 = 10 \text{ pc}$ in front of the *arc*. The γ -ray production rate can then be calculated in the head-on approximation for the interaction cross section. The interested reader will find a brief description of the mathematics in appendix B.

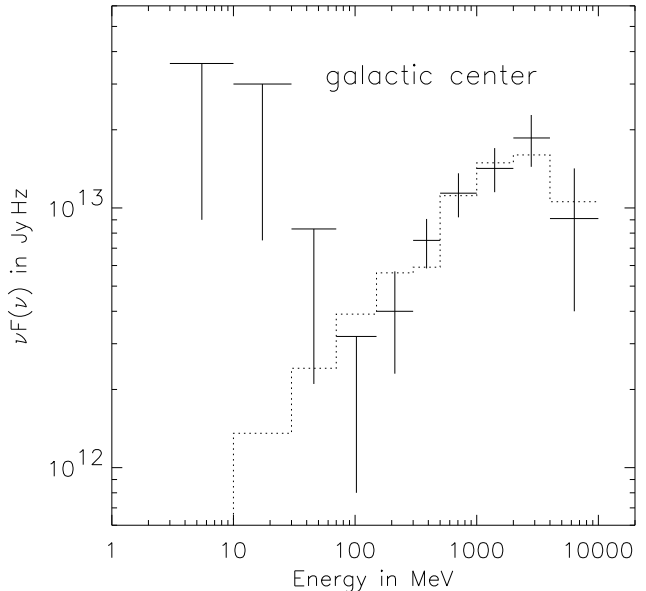


Fig. 2. The spectrum of up-scattered FIR photons from the sickle region in comparison to the γ -ray spectrum of 2EG J1746-2852. The data points represent the differential photon spectrum integrated over the energy bins and multiplied with the geometric mean photon energy of the bin. The EGRET spectrum is taken from Merck et al. (1996), where we have merged some of the low-energy bins. The upper limits are 1σ . An example of the model, for which the input parameters are given in the text, is shown as integral flux per bin in histogram mode.

Given the synchrotron flux at the electron source region, the magnetic field strength in the arc (not in the thin filaments!) and the distance R_0 between the *arc* and the FIR photon source the γ -ray flux is fixed up to a factor of a few. The spatial distribution of synchrotron emission and spectral index, however, depends strongly of the extent of the electron source region. So at present a detail modelling of the synchrotron emission down the southern and northern extensions of the *arc* has the same problems as before in **PRS**: we cannot separate thermal and non-thermal emission, we can hardly determine what part of the non-thermal emission at 4.75 GHz is due to the filaments and what part is due to diffuse emission, and we cannot reliably account for the apparent widening of the *arc*'s cross section with increasing latitude (**PRS**). That is why we cannot reproduce all details in the flux density distribution of the *arc* (Fig.3) and in the spectral index distribution (Fig.4).

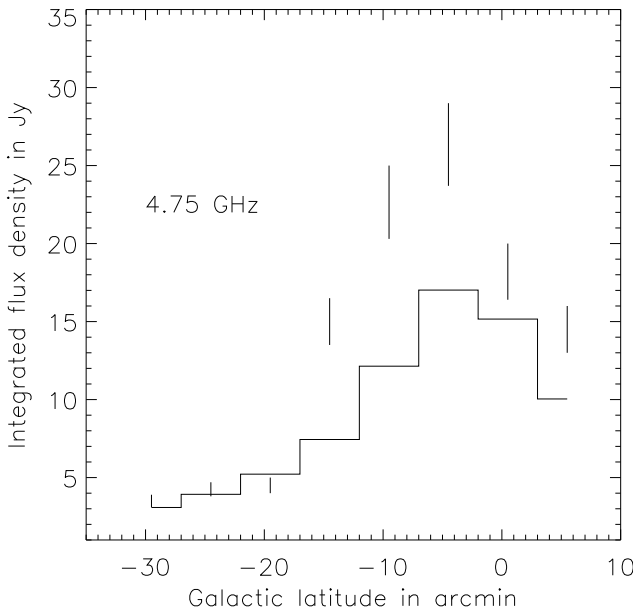


Fig. 3. The predicted radio flux density at 4.75 GHz integrated over the full width of the *arc* and bins of 5 arcmin length in comparison to the data in **PRS**, which are accordingly transformed from the representation in their Table 1b (multiplied with a factor 2.08 times the width of the *arc*). In the inner part of the *arc* the model underpredicts the flux density which is to be expected in view of contributions from thermal emission.

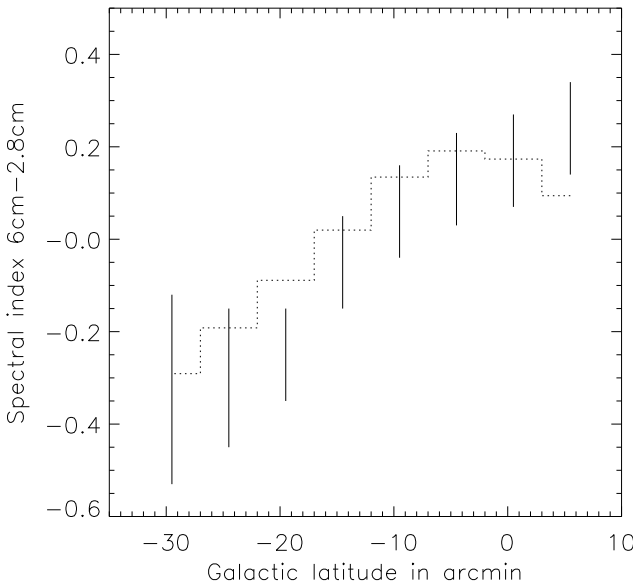


Fig. 4. The predicted spectral index between 4.75 GHz and 10.7 GHz averaged over the full width of the *arc* and bins of 5' length in comparison to the data in **PRS**. In the inner part of the *arc* the observed spectral index may be influenced by contributions from thermal emission.

Given the additional contributions of thermal emission our model should underpredict the radio flux density in the inner part of the *arc*. With this kind of agreement to the radio flux density and spectral index still the basic model reproduces both the flux and the spectrum of the EGRET source 2EG

J1746-2852 correctly, which indicates that the *arc* is likely to be its counterpart. As an example we show in Figs.2-4 the γ -ray spectrum, the distribution of synchrotron flux, and the distribution of radio spectral index for a specific set of parameters. Here the magnetic field strength is taken to be $B = 200\mu G$ in accordance to recent Zeeman splitting data (Uchida and Güsten 1995), the symmetry point of the convection flow is at $b = -4'$, from which the source region of electrons extends 6 pc to negative latitudes and 8 pc in direction of positive latitudes. The injection energy of electrons is $E_0 = 200$ GeV, the turnover frequency ($\nu(E_D)$ in the appendix) between dominance of adiabatic losses and radiative losses is 100 GHz, which then implies that adiabatic losses are nearly four times more effective than losses due to bremsstrahlung ($\eta \simeq 4.7$ in the appendix).

Any other choice for the extent of the source region or the turnover frequency $\nu(E_D)$ affects only the spatial distribution of the low frequency synchrotron emission, and not the γ -ray emission. The integrated synchrotron emission scales mainly with the turn-over frequency.

5. Summary and Discussion

In this paper we have discussed the radio *arc* at the galactic center to be the counterpart of the high-energy γ -ray source 2EG J1746-2852. The observed flux of this source is constant within the statistical limits. The spectrum is very hard and resembles the spectrum of an old pulsar (Merck et al. 1996). Given the typical luminosity of such a pulsar its distance would have to be much less than 1 kpc in distance to produce the observed flux. There is no radio pulsar known compatible in position with 2EG J1746-2852. The chance probability for a Geminga-type object coinciding spatially with the Galactic center is around 10^{-5} , leaving this possibility highly unlikely, although not finally rejectable.

The lack of variability makes it highly unlikely that any of the compact sources in the vicinity of the Galactic Center is the counterpart of 2EG J1746-2852. This includes the peculiar source Sgr A* at the very center of the Galaxy, which is often discussed to harbour a black hole of $10^6 M_\odot$.

We have shown in section 3 and section 4 that the radio *arc* at the galactic center can easily account for the observed properties of 2EG J1746-2852 and is likely to be its counterpart. Existing radio data on the *arc* support the view that its synchrotron emission originates from cooling, initially monoenergetic electrons which diffuse and convect from their sources to the outer extensions of the *arc*. If the source of high-energy electrons coincides with the sickle region, as indicated by the radio data, then the ambient FIR photons can be up-scattered to γ -rays by inverse-Compton interaction with the freshly injected electrons.

We have solved the continuity equation for the electrons including terms for diffusion, convection, monoenergetic injection, and the full energy loss. With that we have shown the predicted γ -ray emission depends mainly on the magnetic field strength in the *arc* and that both the flux and the spectrum of 2EG J1746-2852 can be well explained. A detailed comparison of our model to the spatial variation of synchrotron flux density

and spectral index is, as in earlier work (**PRS**), still hampered by the unknown contributions of thermal emission and the individual filaments which probably have a higher magnetic field strength than the ambient medium. The predicted spatial distribution of synchrotron emission also depends strongly on the spatial extent of the source distribution, in contrast to the prediction for the γ -ray emission. Our model shall be tested on radio data at frequencies beyond 10 GHz in future papers.

Acknowledgements. We like to thank Dr. R. Timmermann for his help on the FIR data of the sickle region. We further thank Michaela Kays for preparing Fig.1.

Appendix A: The particle spectra including complete energy loss terms

The continuity equation for the isotropic differential number density $N(E, z)$ including terms of injection q , energy losses $\beta = -B(E)$, convection with velocity $V = 3V_1 z$, and diffusion with scalar diffusion coefficient $D = D_0 E^a$ can be solved analytically (Lerche and Schlickeiser 1981) under some simplifying conditions.

In case of a point-like source of monoenergetic electrons with energy E_0 , i.e. $q = Q_0 \delta(E - E_0) \delta(z)$ the solution is

$$N(E, z) = \frac{Q_0}{2\sqrt{\pi}} \int_0^\infty dE' \delta(E' - E_0) \Theta(E' - E) \times \frac{\exp(3V_1 \tau(E))}{(V_1 E + B(E))\sqrt{f}} \exp\left[\frac{-z^2 \exp(6V_1 \tau(E))}{4f}\right] \quad (A1)$$

where

$$B(E) = C \left[1 + \frac{E}{E_1} + \frac{E^2}{E_2^2} \right]$$

$$\tau(E) = \int^E du [V_1 u + B(u)]^{-1} = C^{-1} \int^E du \left[1 + \frac{u}{E_1} + \left(\frac{u}{E_2}\right)^2 \right]^{-1}$$

$$f = \int_{\tau(E)}^{\tau(E')} d\tau D_0(\tau) \exp(6V_1 \tau) \quad (A2)$$

The energy loss term $B(E)$ includes ionization and Coulomb losses, nonthermal bremsstrahlung, and synchrotron and inverse Compton interactions. $\tau(E)$ can be readily integrated if $E_2 > 2E_1$, i.e. if $B(E)$ has only real roots. Then

$$\tau(E) \simeq \frac{E_1}{C} \ln \left[\frac{E + E_1}{E + E_D} \right], \quad \text{if } E_D = \frac{E_2^2}{E_1} > 4E_1 \quad (A3)$$

and

$$f = \int_E^{E'} du \frac{D_0 u^a \exp(6V_1 \tau(u))}{C \left(1 + \frac{u}{E_1} + \frac{u^2}{E_2^2} \right)}$$

The cases $E \gg E_1$ have already been solved in an earlier paper (**PRS**), however neglecting bremsstrahlung losses.

New case: $E \ll E_1 \ll E_D$

Here

$$\tau(E) = \frac{2E_1}{C} \ln \left(\frac{E_1}{E_2} \right) \quad (A4)$$

and

$$f(E, E_0) \simeq \frac{D_0 (7\eta - 6)}{C (1 - a)((a + 6)\eta - 6)} E_1^{1-a} E_2^{2a}$$

where

$$\eta = 1 + n_H^{-1} \left(\frac{V_1}{10^{-15} \text{ sec}} \right)$$

is the ratio of adiabatic cooling to bremsstrahlung losses, and finally

$$N(E, z) \simeq \frac{Q_0}{2C} \sqrt{\frac{C(1 - a)((a + 6)\eta - 6)}{D_0 \pi (7\eta - 6)}} \left(\frac{E_1}{E_2} \right)^{6 - \frac{6}{\eta}} \frac{E_1^{(a-1)/2}}{E_2^a} \times \exp\left[-\frac{z^2 C \left(\frac{E_1}{E_2}\right)^{12 - \frac{12}{\eta}} (1 - a)((a + 6)\eta - 6)}{4D_0 E_1^{1-a} E_2^{2a} (7\eta - 6)}\right] \quad (A5)$$

Obviously, the spatial extent of the electron distribution does not depend on energy, and therefore the differential number density has the same energy spectrum as the integrated particle spectrum.

The case $E_1 \ll E \ll E_D$ is given in **PRS** in the limit $\eta \rightarrow \infty$ and has to be changed accordingly. For simplicity we set $a = 0$ throughout the paper.

A simple representation of the energy-dependent scale height is

$$z_c \simeq g(E)^{-1} \sqrt{\frac{DE_1}{C(1 + \frac{E}{E_D})}} \text{ for } E \ll E_0 \quad (A6)$$

$$\text{where } g(E) = \left[\frac{E + E_1}{E + E_D} \right]^{x/2}, \quad x = \frac{6\eta - 6}{\eta} \in [0; 6]$$

The local particle spectrum is thus related to the integral spectrum by

$$N(E, z) \simeq \frac{2N_{tot}(E)}{\sqrt{\pi} z_c(E)} \exp\left[-\frac{z^2}{z_c^2}\right] \quad (A7)$$

where

$$N_{tot} = \frac{Q_0 \Theta(E_0 - E)}{C \left(1 + \frac{E}{E_1} + \frac{E^2}{E_2^2} \right)} \quad (A8)$$

In case the source region is extended to $\pm L$ around $z = 0$ the differential number density writes

$$N(E, z, L) \simeq \frac{N_{tot}(E)}{2L} g(E) \sum_{\pm} \text{erf}\left(\frac{\frac{L}{g(E)} \pm z}{z_c}\right) \quad (A9)$$

More complicated source geometries can also be accounted for by explicit integration over the Green's function (see also Pohl and Schlickeiser 1990).

Appendix B: The production rate of inverse-Compton scattered photons

Here we have to deal with the case of an isotropic electron distribution interacting with a beamed photon distribution, i.e. all photons come from a point-like source.

The differential production rate of γ -rays in the lab frame can be written as

$$S(\epsilon_s, \Omega_s, r) = c \int_0^\infty d\epsilon \oint d\Omega \int_1^\infty d\gamma \oint d\Omega_e (1 - \beta \cos \psi) \times n_e(\gamma, \Omega_e) n_{ph}(\epsilon, \Omega) \left(\frac{d\sigma}{d\epsilon_s d\Omega_s} \right) \quad (B1)$$

where the energies of the incident photon (ϵ) and of the electron (γ) are in units $m_e c^2$, index e refers to the electron, and index s to the final γ -ray. We use the Thomson cross section in head-on approximation

$$\frac{d\sigma}{d\epsilon_s d\Omega_s} = \sigma_T \delta(\Omega_s - \Omega_e) \delta[\epsilon_s - \epsilon \gamma^2 (1 - \beta \cos \psi)] \quad (B2)$$

where the angle between incident and scattered photon directions

$$\cos \psi = \mu \mu_e + \sqrt{1 - \mu^2} \sqrt{1 - \mu_e^2} \cos(\phi - \phi_e) \quad (B3)$$

is related to the incident photon and electron directions ($\mu_x = \cos \theta_x$).

While the electron distribution is isotropic

$$n_e(\gamma, \Omega_e) = \frac{n_e(\gamma)}{4\pi} \quad (B4)$$

the target photon density is beamed

$$n_{ph}(\epsilon, \Omega) = n_{ph}(\epsilon) \delta(\phi) \delta(\mu - 1) \quad (B5)$$

After some simple algebra we obtain the γ -ray production rate in direction μ_s

$$S(\epsilon_s, \mu_s, r) = \frac{c \sigma_T}{4\pi} \int_1^\infty d\gamma \frac{n_e(\gamma)}{\gamma^2} n_{ph} \left(\frac{\epsilon_s}{\gamma^2 (1 - \beta \mu_s)} \right) \quad (B6)$$

Let the photon source be located at a distance R_0 to the *arc* in front of it. The total γ -ray emissivity is then derived by integration over the length of the *arc* where at each position μ_s is the cosine of the angle between the line-of-sight to the observer and the direction to the photon source, and the target photon density is related to the total FIR luminosity of the illuminating molecular cloud M0.20-0.033

$$n_{ph}(\epsilon) = \frac{L_{FIR} \mu_s^2}{6.5 (kT)^2 4\pi R_0^2 c} \left(\frac{\epsilon}{kT} \right)^2 \frac{1}{\exp \left(\frac{\epsilon}{kT} \right) - 1} \quad (B7)$$

with the temperature T fixing the grey-body spectrum.

References

Anantharamiah K.R., Pedlar A., Ekers R.D., Goss W.M.: 1991, MNRAS 249, 262

Churazov E., Gilfanov M., Sunyaev R. et al.: 1994, ApJS 92, 381

Goldwurm A., Cordier B., Paul J. et al.: 1994, Nat 371, 589

Kaastra J.S.: 1985, PhD Thesis, University of Utrecht

Kanbach G., Bertsch D.L., Favale A. et al.: 1988, Space Sci. Rev. 49, 69

Krichbaum T.P., Schalinski C.J., Witzel A. et al.: 1994, in *Nuclei of normal galaxies: Lessons from the Galactic Center*, Eds. R. Genzel, Kluwer, Dordrecht

Lasenby J., Lasenby A.N., Yusef-Zadeh F.: 1989, Proc. IAU Symposium 136, Ed. M. Morris, Kluwer, Dordrecht, p.293

Lerche I., Schlickeiser R.: 1981, ApJS 47, 33

Melia F.: 1994, ApJ 426, 577

Mastichiadis A., Ozernoy L.: 1994, ApJ 426, 599

Mattox J.R., Bertsch D.L., Chiang J. et al.: 1996, ApJ in press

Merck M., Bertsch D.L., Dingus B.L. et al.: 1996, A&AS submitted

Morris M., Davidson J.A., Werner M.W.: 1995, in *Airborne Astronomy Symposium on the Galactic Ecosystem*, Eds. M.R. Haas, J.A. Davidson and E.F. Erickson, ASP Conference Series, Vol.73, p.477

Narayan R., Yi I., Mahadevan R.: 1996, A&AS, in press

Odenwald S.F., Fazio G.G.: 1984, ApJ 283, 601

Pohl M., Schlickeiser R.: 1990, A&A 234, 147

Pohl M., Reich W., Schlickeiser R.: 1993, A&A 262, 441 (PRS)

Predehl P., Trümper J.: 1994, A&A 290, L29

Reich W., Sofue Y., Wielebinski R., Seiradakis J.H.: 1988, A&A 191, 303

Reich W.: Proc. IAU Symposium 140, Eds. R. Beck et al., Kluwer, Dordrecht, p.369

Schlickeiser R.: 1984, A&A 136, 227

Serabyn E., Morris M.: 1994, ApJ 424, L91

Skinner G.K., Willmore A.P., Eyles C.J. et al.: 1987, Nat 330, 544

Sofue Y., Murata Y., Reich W.: 1992, PASJ 44, 367

Sofue Y.: 1995a, PASJ 47, 527

Sofue Y.: 1995b, PASJ 47, 551

Strong A.W., Bennett K., Bloemen H. et al.: 1994, A&A 292, 82

Sunyaev R., Pavlinskii M., Gilfanov M. et al.: 1991, Sov. Astron. Lett. 17(1), 42

Taylor J.H., Manchester R.N., Lyne A.G.: 1993, ApJS 88, 529

Thompson D.J., Bertsch D.L., Fichtel C.E. et al.: 1993, ApJS 86, 629

Thompson D.J., Bertsch D.L., Dingus B.L. et al.: 1996, ApJ in press

Tsuboi M., Kawabata T., Kasuga T. et al.: 1995, PASJ 47, 829

Uchida K.I., Güsten R.: 1995, A&A 298, 473